

## 7.1 MULTI-DIMENSIONAL BROADBAND IR RADIATIVE FORCING OF MARINE STRATOCUMULUS IN A LARGE EDDY SIMULATION MODEL

David B. Mechem<sup>1</sup>, Mikhail Ovtchinnikov<sup>2</sup>, Yefim L. Kogan<sup>1</sup>, Anthony B. Davis<sup>3</sup>, Robert F. Cahalan<sup>4</sup>, Ezra E. Takara<sup>5</sup>, and Robert G. Ellingson<sup>5</sup>

<sup>1</sup>Cooperative Institute for Mesoscale Meteorological Studies, University of Oklahoma, Norman, Oklahoma

<sup>2</sup>Pacific Northwest National Laboratory, Richland, Washington

<sup>3</sup>Los Alamos National Laboratory, Los Alamos, New Mexico

<sup>4</sup>NASA/Goddard Space Flight Center, Greenbelt, Maryland

<sup>5</sup>Florida State University, Tallahassee, Florida

### 1. INTRODUCTION\*

Marine boundary layer clouds profoundly influence the global shortwave radiation budget through their effect on albedo, but a significant source of turbulent energy to the boundary layer and the clouds themselves is longwave cloud top cooling. Cloudy regions can be thought of as radiating as blackbodies in the longwave, with a net radiative flux of nearly zero inside the cloud itself and a significant radiative flux divergence within a few tens of meters of the cloud edge.

Current large eddy simulation (LES) models use radiative transfer (RT) schemes that consider photon transport in one direction only. Using these plane-parallel methods seems reasonable for clouds like stratocumulus that are to a large degree horizontally uniform, but close inspection of these clouds shows marked undulations in cloud top: billows and valleys that arise from the turbulent overturning of the boundary layer. Guan et al. (1995) show that horizontal photon transport interacts with these cloud top perturbations to produce a heating rate distribution different from that of a horizontally uniform cloud. The effect of the undulations is to reduce mean cloud top radiative forcing, but the local distribution of the cooling implies a positive feedback on the maintenance of the turbulent eddies themselves. This result seems somewhat paradoxical and does not address what the ultimate effect of the radiative-dynamic interaction might be. Guan et al. (1997) document an interaction between multi-dimensional radiative transfer and cloud dynamics for a small, slab-symmetric cumulus. Longwave cooling on the sides of the cloud strengthens the convective downdraft and enhances convergence at cloud base, promoting further cloud development.

It is clear that applying incorrect radiative forcing to a numerical model has the potential to lead to a bias in model behavior. Results from the Intercomparison of 3D Radiation Codes (I3RC) project show that the plane-parallel assumption is often unwarranted and can lead to

significant errors in mean heating rates. Although the majority of the I3RC efforts to date have concentrated on the shortwave part of the spectrum, many of the results seem to be similarly applicable to longwave.

To explore this issue for boundary layer clouds, we have coupled to an LES the sophisticated multi-dimensional radiative transfer scheme of Evans (1998; Spherical Harmonics Discrete Ordinate Method — SHDOM). This computational framework enables us to address the interactive and evolutionary nature of the radiative-dynamic interaction and quantify its importance.

### 2. METHODOLOGY

The Cooperative Institute of Mesoscale Meteorological Studies (CIMMS) LES (Kogan et al. 1995; Khairoutinov and Kogan 1999) is coupled with SHDOM in an interactive fashion. The LES supplies the cloud field to SHDOM, which calculates cloud optical properties and then uses a correlated k-distribution to compute RT in 12 bands from 4-100  $\mu\text{m}$ . The calculation includes emission, absorption, and scattering effects. Scattering is often assumed to be insignificant for longwave radiation, leading to a simplified computation of RT. This assumption is unnecessary using SHDOM, since scattering is calculated by simple (and numerically inexpensive) multiplication in spherical harmonic space.

Two cases are simulated. The first is a lightly drizzling deck of unbroken stratocumulus. In contrast to the first, the second case represents a clean maritime air mass that produces prodigious drizzle and a broken cloud field. Initial conditions for the LES are similar to the subtropical Atlantic case (ASTEX A209) simulated by Khairoutdinov and Kogan (1995). Horizontal and vertical grid spacings are 100 m and 25 m, respectively, and lateral boundary conditions are periodic. Surface fluxes of heat and moisture are  $10 \text{ Wm}^{-2}$  and  $25 \text{ Wm}^{-2}$ . CCN concentrations are distributed lognormally and are  $290 \text{ cm}^{-3}$  and  $41 \text{ cm}^{-3}$  in the unbroken and clean (drizzling) cases, respectively. The RT calculates droplet radius based on a concentration of  $50 \text{ cm}^{-3}$  and assumes a U. S. Standard Atmosphere thermodynamic profile.

Because of computational expense, all simulations are two-dimensional. Since it is only a small fraction of the computational total compared to the RT calculation, explicit (bin) microphysical processes are used. The

---

\*Corresponding author address: David Mechem, Cooperative Institute for Mesoscale Meteorological Studies, University of Oklahoma, 100 E. Boyd, Room 1110, Norman, OK 73019. Email: dmechem@ou.edu

model is run for an hour using its own (1D) RT scheme to establish reasonable boundary layer structure. Then, simulations are performed using the coupled LES-SHDOM model, one with the full multi-dimensional treatment of RT, and the other under the independent pixel approximation (IPA) mode of SHDOM. The RT calculation is performed every 40 seconds rather than every timestep as is usually done in LES computations. Compared to calculating RT every timestep, we estimate the RMS error to be  $\sim 3\%$  for the lightly drizzling case. For the strongly drizzling case, RMS error approaches 9% late in the simulation when significant variability is present in the cloud field. The first case is performed using a domain size of  $500 \times 51$  and is run for two hours. The strongly drizzling run must be run for five hours to experience significant cloud breakup, and its domain is reduced to  $100 \times 51$  to keep computational time reasonable.

### 3. LIGHTLY DRIZZLING SCENARIO (CASE 1)

Two simulations of case 1 are compared, MDRT and IPA. The curves in Figure 1 can be thought of as a proxy for mean cloud top LW forcing and variability. The average column peak cooling rate is reduced in the MDRT case by  $0.3\text{--}0.4 \text{ K h}^{-1}$  compared to the IPA simulation. This difference is consistent over the course of the simulation, while the variability (as measured by the standard deviation error lines) is largely similar in both runs.

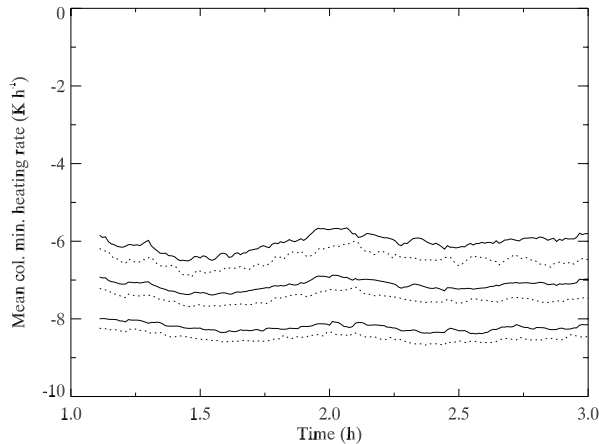


*Figure 1.* Time series of domain-averaged column peak heating rate for MDRT (solid line) and IPA (dotted line). Lines for one standard deviation about the means are also plotted.

Figure 2a shows a 5 km segment of the 50 km domain at 3 h. Average cloud depth is approximately 430 m, with maximum liquid water content (LWC) values of  $0.7 \text{ g kg}^{-1}$ . Significant horizontal variability is readily apparent at cloud top, in the cloud interior, and at cloud base. A magnified portion of the top of the cloud is pre-

sented in Figure 2b, showing more clearly the cloud top peaks and valleys. Contours of horizontal radiative flux ( $F_x$ ) for the atmospheric LW window are overlaid on the liquid water field. We assume that the flux vectors for this single band are at least qualitatively representative of the broadband flux. Flux vectors more completely represent the total radiative effect, but the sharp flux gradient at cloud top renders them less useful than for the typical shortwave situation. Regions of significant  $F_x$  are associated with cloud top undulations. Visually,  $F_x$  is proportional to the horizontal gradient in LWC but only near undulating regions. Horizontal structure in LWC without the corresponding cloud top variability (e.g. from  $x = 10\text{--}10.75 \text{ km}$  in Fig. 2b) produces little net horizontal photon transport. Because of the blackbody nature of the cloud,  $F_x$  strongly attenuates with cloud depth, though the model shows large values frequently penetrating to a cloud depth nearly double that of the cloud top perturbations.

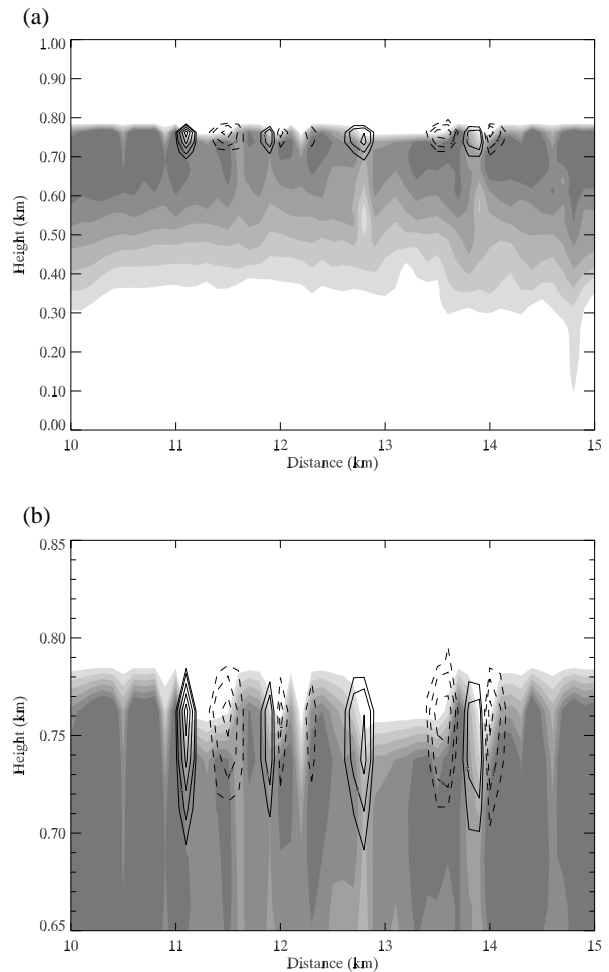


*Figure 2.* (a) Liquid water field and  $10.2\text{--}12.5 \mu\text{m}$  band horizontal radiative flux over a subset of the 50 km model domain at 3 h. Contour intervals are  $0.1 \text{ g kg}^{-1}$  for liquid water and  $1.0 \text{ W m}^{-2}$  for horizontal radiative flux. (b) Magnified portion of the cloud top.

The net consequence of these local horizontal radiative fluxes is to produce the effect shown in Figure 1, a reduced mean cooling profile compared to a plane-parallel treatment of RT. Guan et al. (1995) explain this phenomenon as the anomalous warming in the “valley” regions being greater than the anomalous cooling in the “ridge” regions.

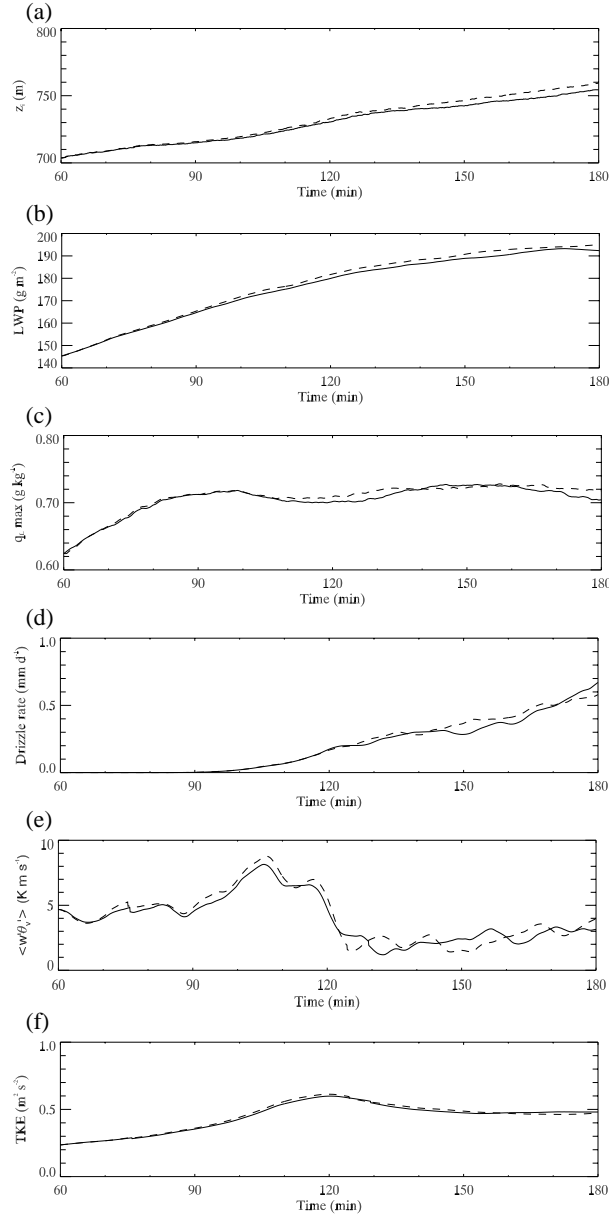


**Figure 3.** Time series of various mean LES quantities from 1-3 h for the lightly drizzling simulation. The solid lines are MDRT, and dashed lines are IPA RT. (a) Inversion height; (b) Liquid water path; (c) Maximum liquid water content; (d) Surface drizzle rate; (e) Buoyancy flux; (f) Turbulent kinetic energy.

The interactive MDRT-dynamic effect for CASE 1 can be seen in Figure 3. The comparisons between MDRT and IPA show a subtle but systematic bias in

these boundary layer metrics. Entrainment as measured by the cloud top height over the two hours is 9.5% higher in the IPA experiment. This is physically plausible, since reduced cloud top radiative forcing should decrease the strength of the eddies and ultimately reduce the entrainment, although the local distribution of the forcing might produce a response more complicated than a simple reduction in mean cloud top cooling. Liquid water path (LWP) is 5.6% greater in the IPA results — somewhat counterintuitive, though boundary layer sensitivities are often highly nonlinear. We speculate that the weaker forcing results in diminished vertical moisture flux in the MDRT case, leading to slightly less LWP. For much of the simulation, the maximum liquid water path is greater in the IPA case, but the bias in drizzle rate, buoyancy flux, and TKE actually switches signs over the two hours. One possible explanation for this is the effect of the light drizzle. The IPA case initially produces more drizzle, which falls and cools the subcloud layer, reducing TKE and buoyancy flux. Drizzle production and entrainment then decrease. Stevens (1999) terms this type of feedback a “rigidity on the flow,” which is symptomatic of a decreased sensitivity to experimental parameters. This subtle feedback between radiative forcing, entrainment, boundary layer energy, and precipitation process should be expected to decrease when drizzle is not produced.

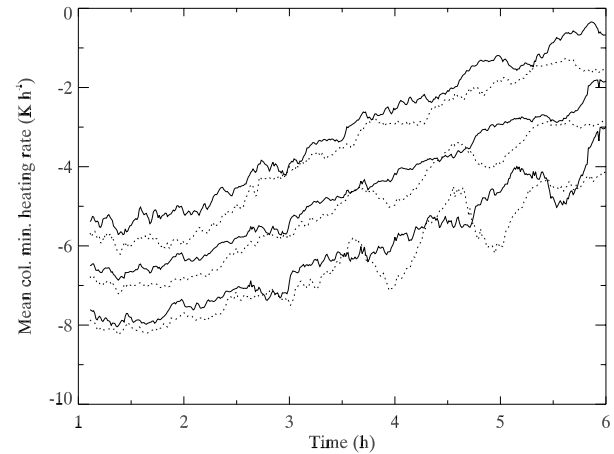


**Figure 4.** Time series of domain-averaged column peak heating rate from 1-6 h for the strongly drizzling MDRT (solid line) and IPA (dotted line) simulations. Lines for one standard deviation about the means are also plotted.

#### 4. HEAVILY DRIZZLING SCENARIO (CASE 2)

When the initial CCN concentration is reduced from  $290 \text{ cm}^{-3}$  to  $41 \text{ cm}^{-3}$ , the LES produces strong drizzle and a temporal transition from unbroken stratocumulus to a broken, boundary layer cumulus regime. As in the unbroken case, the MDRT cooling rates (Figure 4) are smaller than those calculated using the IPA, though both steadily decrease with time (less cloud top cooling). This

trend in the heating rate results from the decrease with time of cloud fraction and the much smaller peak cooling rates in the clear regions compared to the cloudy regions. For both case 1 and 2, this quantity can be thought of as being proportional to column LW radiative forcing in a mesoscale or NWP model. The signal is noisier than for case 1 because of strong temporal evolution and the fact that the domain is only 20% as large. The tops of the broken clouds themselves have a cooling signal similar in magnitude to the solid clouds in case 1, which explains why the variability (standard deviation lines) differs little between the two cases.

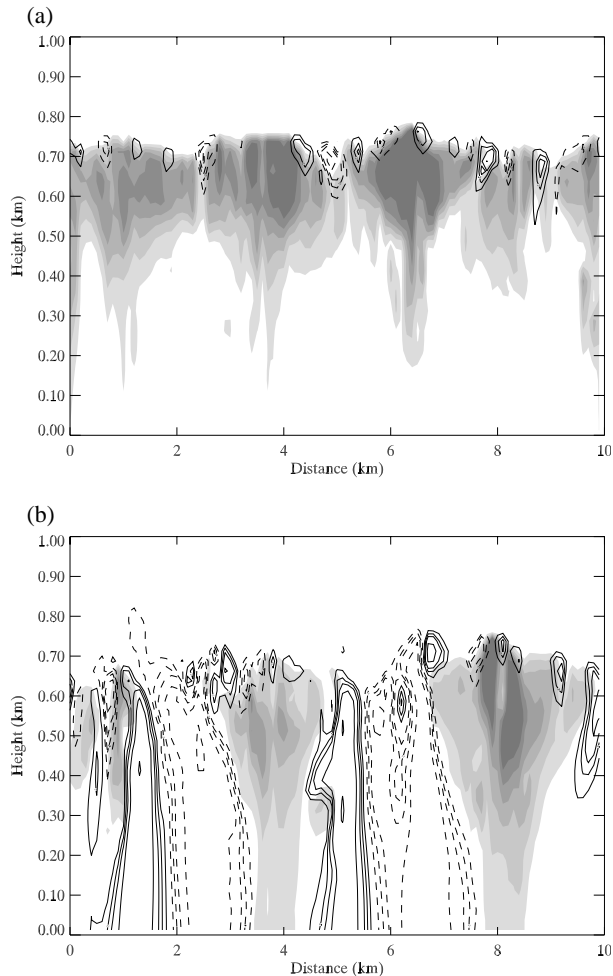


**Figure 5.** Liquid water field and 10.2-12.5  $\mu\text{m}$  band horizontal radiative flux at 3 h for the strongly drizzling MDRT case. (a) 3 h; (b) 5 h. Contour intervals are 0.1  $\text{g kg}^{-1}$  for liquid water. Radiative flux contour levels are  $\pm 15, \pm 10, \pm 5, \pm 3, \pm 2$ , and  $\pm 1 \text{ W m}^{-2}$ .

Figure 5a shows that variation in cloud top structure is greater in the strongly drizzling simulation (case 2) than in case 1. The horizontal fluxes located near cloud top are qualitatively similar though somewhat larger locally than in case 1. Although cloud base varies considerably over the domain, the net horizontal flux associ-

ated with the cloud base variations is negligible, indicating that the cloud base regions are nearly in radiative equilibrium. The horizontal fluxes only become appreciable after 5 h (Fig. 5b) when the cloud begins to break apart, implying that the fluxes are predominantly associated with the interaction of the broken clouds with the upwelling LW radiation from the surface. Horizontal fluxes in the cloud-free regions contribute very little radiative forcing since the flux divergence is quite small, so the difference between MDRT and IPA seems mostly confined to regions near cloud top, just as was the case in the unbroken cloud. This finding is somewhat different from that of Guan et al. (1997) who found weak, systematic cooling on the sides of a cumulus cloud. Their cloud was an isolated cumulus, whereas the clouds in case 2 are separated by clear regions that are approximately the same scale as that of the cloud itself. It is conceivable that the sides of the closely spaced clouds are in radiative equilibrium but that net cooling results when the spacing between is increased.

The evolution of various boundary layer quantities for case 2 is shown in Figure 6. The inversion height is omitted because cloud breakup makes its calculation somewhat problematic, although comparing Figs. 2a and 5a shows that the strong drizzle case entrains less, as would be expected. The statistics are noisy compared to those for case 1, likely a result of the smaller domain. The presence of drizzle adds to the large degree of variability, as the pulses in surface drizzle rate are also reflected in LWP, maximum liquid water, and buoyancy flux. This variability is related to the lifetime of the drizzle cells and is emphasized in the small domain where only one or two cells are simultaneously present. Smoothing of the curves shows a result similar to case 1, namely that reducing slightly the net LW forcing reduces boundary layer energetics and drizzle production.

## 5. CONCLUSIONS

We have attempted to identify the existence of an evolutionary bias arising from the use the plane-parallel assumption in forcing a large eddy simulation of marine stratocumulus. The bias in the case of lightly drizzling, unbroken cloud is subtle but seems systematic. Because there are indications that the presence of drizzle may damp somewhat the response to the change in forcing, a non-drizzling situation should be investigated in addition to those cases discussed here.

Computational expense ultimately places limits on the conclusions that can be drawn from case 2. The differences in evolution are more noisy but appear to be slightly greater using MDRT compared to IPA. Unfortunately, the RMS error of applying the RT calculation every 40 s is approximately 9%, which is only slightly less than the difference between MDRT and IPA for this case. A larger domain run with less time between RT calculations would perhaps shed more light on the broken cloud scenario.

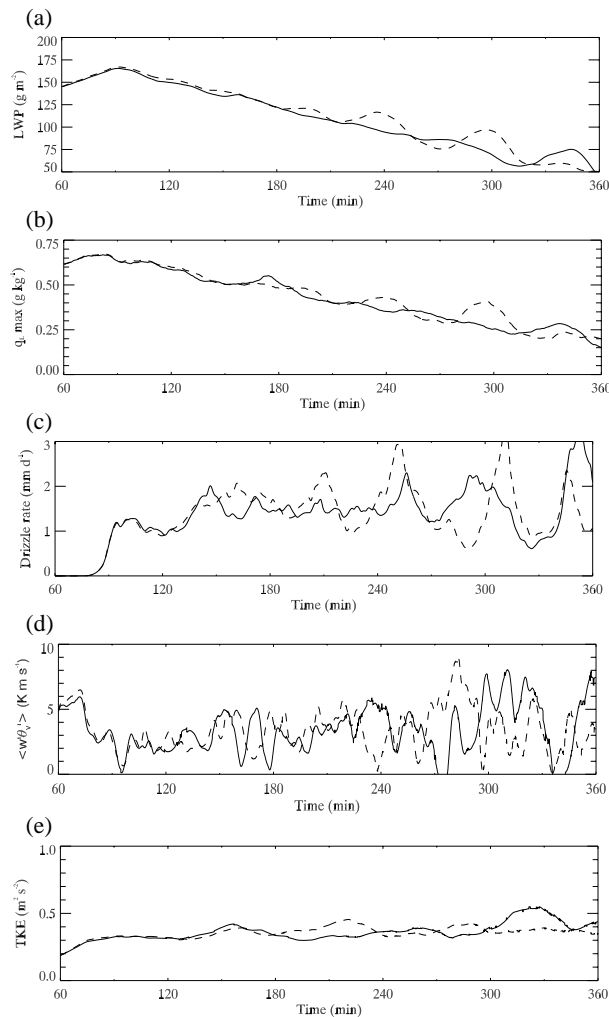


Figure 6. Time series of various mean LES quantities from 1-6 h for the heavily drizzling, broken cloud field simulation. The solid lines are MDRT, and dashed lines are IPA RT. (a) Liquid water path; (b) Maximum liquid water content; (c) Surface drizzle rate; (d) Buoyancy flux; (e) Turbulent kinetic energy.

These systematic longwave responses, though subtle, could conceivably lead to pronounced shortwave radiative consequences. For the examples in this study, the more realistic treatment of RT (MDRT) reduces entrainment and associated drying of the cloud layer. This typically produces a more persistent cloud feature and higher albedo values, ultimately resulting in a larger global cooling effect. The response is nonlinear and highly speculative, however, as drastically reducing the radiative forcing will not monotonically increase cloud persistence; rather, the boundary layer energetics would reduce the vertical moisture transport to the degree that the cloud might dissipate.

Two issues of model resolution need to be explored. First, the simulations are performed using a vertical grid spacing of 25 m, while the undulations in cloud top in

Figure 2 are of this same scale. Since the undulations are where the multi-dimensional RT effect seems to happen, resolving them adequately is highly important. The quality of the heating rates calculated by the RT scheme depends upon how finely specified the liquid water field is. In addition, too crude of a grid spacing at cloud top can lead to a pronounced overestimate of entrainment suggested by Stevens et al. (1999). We acknowledge that the possibility of an overestimate in these simulations but claim that it would have little impact on the relative difference between the two simulations. The second resolution concern to be addressed is how adequate an angular resolution is necessary to produce accurate heating rates. Calculations of fluxes and heating rates typically require less angular resolution than is needed for radiances, but this issue needs to be explored further. Testing these resolution dependencies can be accomplished by performing RT calculations on single cloud fields; the full interactive model is unnecessary.

## 6. ACKNOWLEDGEMENTS

This research was supported by the Environmental Sciences Division of the U. S. Department of Energy (through Battelle PNR Contract 144880-A-Q1 to the Cooperative Institute for Mesoscale Meteorological Studies) as part of the Atmospheric Radiation Measurement Program, and by ONR N00014-96-1-0687 and N00014-96-1-1112. Lan Yi provided support with the LES model.

## 7. REFERENCES

- Evans, K. F., 1998: The spherical harmonics discrete ordinate method for three-dimensional atmospheric radiative transfer. *J. Atmos. Sci.*, **55**, 429-446.
- Guan, H., R. Davies, and M. K. Yau, 1995: Longwave radiative cooling rates in axially symmetric clouds. *J. Geophys. Res.*, **100**, 3213-3220.
- Guan, H., M. K. Yau, and R. Davies, 1997: The effects of longwave radiation in a small cumulus cloud. *J. Atmos. Sci.*, **54**, 2201-2214.
- Khairoutdinov, M. P., and Y. L. Kogan, 1999: A large eddy simulation model with explicit microphysics: Validation against aircraft observations of a stratocumulus-topped boundary layer. *J. Atmos. Sci.*, **56**, 2115-2131.
- Kogan, Y. L., M. P. Khairoutdinov, D. K. Lilly, Z. N. Kogan, and Q. Liu, 1995: Modeling of stratocumulus cloud layers in a large eddy simulation model with explicit microphysics. *J. Atmos. Sci.*, **52**, 2923-2940.
- Stevens, B., C.-H. Moeng, and P. P. Sullivan, 1999: Large-eddy simulations of radiatively driven convection: Sensitivities to the representation of small scales. *J. Atmos. Sci.*, **56**, 3963-3983.